Continuous versus Arrested Spreading of Biofilms at Solid-Gas Interfaces: The Role of Surface Forces

Sarah Trinschek,[1,2,3] Karin John,[2,3] Sigolène Lecuyer,[2,3] and Uwe Thiele[1,4,*]
[1]Institut für Theoretische Physik, Westfälische Wilhelms-Universität Münster, Wilhelm-Klemm-Strasse 9, 48149 Münster, Germany
[2]Université Grenoble Alpes, LIPHY, F-38000 Grenoble, France
[3]CNRS, LIPHY, F-38000 Grenoble, France
[4]Center of Nonlinear Science (CeNoS), Westfälische Wilhelms-Universität Münster, Corrensstrasse 2, 48149 Münster, Germany

(Received 20 December 2016; revised manuscript received 25 April 2017; published 16 August 2017)

We introduce and analyze a model for osmotically spreading bacterial colonies at solid-air interfaces that includes wetting phenomena, i.e., surface forces. The model is based on a hydrodynamic description for liquid suspensions which is supplemented by bioactive processes. We show that surface forces determine whether a biofilm can expand laterally over a substrate and provide experimental evidence for the existence of a transition between continuous and arrested spreading for *Bacillus subtilis* biofilms. In the case of arrested spreading, the lateral expansion of the biofilm is confined, albeit the colony is biologically active. However, a small reduction in the surface tension of the biofilm is sufficient to induce spreading. The incorporation of surface forces into our hydrodynamic model allows us to capture this transition in biofilm spreading behavior.

DOI: 10.1103/PhysRevLett.119.078003

Biofilms are macrocolonies of bacteria enclosed in an extracellular matrix that form at diverse interfaces [1]. Cell proliferation and matrix production by the bacteria result in lateral spreading of the colony along the interface. Surprisingly, during the osmotic spreading of biofilms on moist solid (agar) substrates in contact with a gas phase, the spreading is not driven by the active motility of individual bacteria but hinges on the physicochemical properties of the biofilm and the interfaces [2–4]. Within this mechanism, the biological production of polymeric matrix results in an osmotic flux of water from the agar into the biofilm that subsequently swells and spreads out. As the spreading involves the motion of a three-phase contact line between the viscous biofilm, the agar, and the gas phase, wetting phenomena [5,6] are likely to play an important role. This idea is supported by experiments that indicate a strong dependence of biofilm spreading on their ability to produce biosurfactants [7–13]. In this Letter, we present a modeling approach which explicitly includes surface forces in order to understand their role in biofilm spreading behavior.

To demonstrate the effect of surfactants, we perform osmotic biofilm spreading experiments using a *Bacillus subtilis* wild-type strain NCIB 3610 (WT) and a mutant strain with deficient production of surfactin ($\Delta srfAA$)—a natural biosurfactant produced by WT *B. subtilis*. Typically, production is induced at a high cell density by cell-to-cell communication (quorum sensing) [14,15] and plays a key role in surface motility [16,17]. Bacterial suspensions and agar substrates are prepared as described in Supplemental Material [18]. Agar plates with an appropriate nutrient medium are inoculated with a small droplet of the cell suspension, and biofilm growth and spreading is subsequently monitored. Figures 1(a) and 1(b) show the colony of the WT and the mutant strain, respectively, after 3 days of incubation. Growth curves and further images of days 1 and 2 can be found in Ref. [18]. The WT in (a) expands with a rate of 0.2 mm/h and forms circular biofilms with a diameter of about 2 cm, whereas the mutant strain without surfactin in (b) is not able to spread. The external addition of surfactin shortly after agar inoculation has no effect on the spreading of the WT strain [Fig. 1(c)] but restores a WT morphology in the surfactin-deficient strain [Fig. 1(d)]. The WT phenotype can

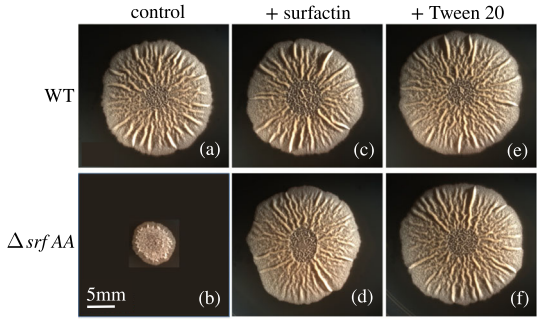

FIG. 1. Experimental observation of the influence of surfactants on the transition between continuous and arrested biofilm spreading. (a) The *B. subtilis* WT spreads laterally with a velocity of 0.2 mm/h over the agar substrate, whereas (b) for the mutant strain with deficient surfactin production ($\Delta srfAA$) spreading is arrested. An external addition of the surfactants (c),(d) surfactin or (e),(f) Tween 20 enables the mutant strain to spread but does not affect the WT.

also be recovered by adding the nonphysiological surfactants Tween 20 [Figs. 1(e) and 1(f)] or Span80 (not shown), which points at a physical role of surfactin in the spreading mechanism.

To model the influence of wetting phenomena on biofilm spreading, we supplement a hydrodynamic description of a thin film of a biologically passive liquid suspension [19–21] by biomass growth processes. In general, the aspect of physical surface forces has up to now found only little attention in the otherwise very rich literature concerning the mathematical models for biofilms which are diverse in the modeling approaches used and the processes considered (for reviews, see, for example, [22–25]). The recently introduced model [26] explicitly includes surface forces, i.e., wettability, via a Derjaguin (or disjoining) pressure and capillarity via the interface tensions. Similar thin film models without wettability influences are used to study early-stage biofilm growth and quorum sensing [27], osmotically driven spreading [2], and the effect of surfactant production on the spreading of a bacterial colony up a non-nutritive wall [11].

Here, a biofilm of height $h(x,y,t)$ is modeled as a mixture of solvent (nutrient-rich water) and of biomass (bacteria and extracellular polymeric matrix) with the height-averaged biomass concentration $\phi(x,y,t)$ (see Fig. 2). The free energy functional that determines all transport processes for the passive suspension is

$$F[h,\phi] = \int \left[f_w(h) + h f_m(\phi) + \frac{\gamma}{2}(\nabla h)^2 \right] dA, \quad (1)$$

where γ is the biofilm-air surface tension and $\nabla = (\partial_x, \partial_y)^T$ is the planar gradient operator, while γ_{SG} and γ_{SL} denote the solid-gas and solid-liquid interface energies. A common choice for the wetting energy is [6,28]

$$f_w(h) = A\left(-\frac{1}{2h^2} + \frac{h_p^3}{5h^5} \right), \quad (2)$$

which combines destabilizing long-range van der Waals and stabilizing short-range interactions. Here, h_p denotes the height of a thin wetting layer and

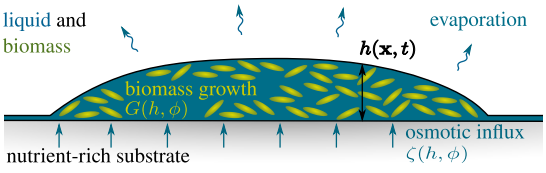

FIG. 2. Sketch of the osmotically driven spreading of a biofilm with the height profile $h(\mathbf{x},t)$. Osmotic pressure gradients are generated as bacteria consume water and nutrients to produce biomass via bacterial proliferation and matrix secretion, which is described by the growth term $G(h,\phi)$. This causes an osmotic influx of nutrient-rich water $\zeta(h,\phi)$ from the moist agar substrate into the biofilm.

$$A = \frac{10}{3} h_p^2 (\gamma - \gamma_{SG} + \gamma_{SL}) \quad (3)$$

is the Hamaker constant, here expressed through the interface energies. For a partially wetting biofilm-substrate-air combination, minimizing Eq. (1) gives the coexistence of a wetting layer of height h_p with steady droplets of equilibrium contact angle $\cos\theta_{eq} = 1 + f_w(h_p)/\gamma = (\gamma_{SG} - \gamma_{SL})/\gamma$, equivalent to the Young-Dupré equation [5]. The film bulk contribution

$$f_m(\phi) = \frac{k_B T}{a^3} [\phi \ln(\phi) + (1-\phi)\ln(1-\phi)] \quad (4)$$

represents the entropic free energy of mixing of the solute and solvent. We assume, for simplicity, that the biomass and solvent are represented by the same microscopic length a. $k_B T$ denotes the thermal energy.

The passive convective flux $\mathbf{j}_{conv}$ and diffusive flux $\mathbf{j}_{diff}$ are derived by applying a variational principle to the free energy (1) (for details, see [21,26]):

$$\mathbf{j}_{conv} = \frac{h^3}{3\eta} \nabla(\gamma \Delta h - \partial_h f_w), \quad (5)$$

$$\mathbf{j}_{diff} = -D_{diff} h \phi \nabla(\partial_\phi f_m). \quad (6)$$

The composition-dependent viscosity η of the biofilm [29–31] is given by $\eta = (1-\phi)\eta_0 + \phi\eta_b$, where η_0 and η_b denote the viscosity of the solvent and biomass, respectively. The biomass diffusivity is $D = (a^2/6\pi\eta)$, consistent with the diffusion constant $D_{diff} = D(k_B T/a^3) = (k_B T/6\pi a \eta)$.

The biomass multiplies by consuming nutrient-rich water following a bimolecular reaction $g\phi(1-\phi)$ with the growth rate constant g. To account for processes such as nutrient and oxygen depletion [3,32], we introduce a limiting biomass amount $\phi_{eq} h^\star$ that corresponds to the maximum which can be sustained per substrate area. It is related to the thickness for which nutrient diffusion and consumption of nutrients by the bacteria throughout the vertical profile of the film equilibrate [27]. We assume a simple logistic growth law

$$G(h,\phi) = g\phi(1-\phi)\left(1 - \frac{h\phi}{\phi_{eq} h^\star}\right) f_{mod}(h,\phi), \quad (7)$$

where $f_{mod}(h,\phi)$ modifies the growth law locally for very small amounts of biomass as defined in Ref. [33]. It ensures that at least one bacterial cell is needed for cell division and, thus, proliferation of biomass does not take place in the wetting layer.

Since the biomass cannot diffuse into the agar, biomass growth creates an osmotic imbalance between the biofilm and the agar. We assume that the agar constitutes a large reservoir of nutrient-rich water at a constant osmotic pressure μ_{agar}, corresponding to an equilibrium water concentration $(1-\phi_{eq})$ in a flat biofilm. The osmotic

pressure in the biofilm, defined as the negative of the variation of the free energy (1) with respect to the height h at a fixed number of osmotically active particles $h\phi$, is given by

$$\mu_s = -\frac{\delta F[h,\phi]}{\delta h} + \frac{\phi}{h}\frac{\delta F[h,\phi]}{\delta \phi} = -\partial_h f_w - f_m + \phi \partial_\phi f_m + \gamma \Delta h. \quad (8)$$

The osmotic flux of water between the agar and biofilm depends linearly on the osmotic pressure difference, $\zeta(h,\phi) = Q_{\mathrm{osm}}(\mu_s - \mu_{\mathrm{agar}})$, with Q_{osm} being a positive mobility constant.

Biomass growth and osmotic flux are incorporated into the model as two nonconserved terms $G(h,\phi)$ and $\zeta(h,\phi)$, which results in the following evolution equations for the effective layer thicknesses of liquid h and biomass $h\phi$:

$$\partial_t h = -\nabla \cdot \mathbf{j}_{\mathrm{conv}} + \zeta(h,\phi), \quad (9)$$

$$\partial_t (h\phi) = -\nabla \cdot (\phi \mathbf{j}_{\mathrm{conv}} + \mathbf{j}_{\mathrm{diff}}) + hG(h,\phi). \quad (10)$$

Note that the conserved part of the dynamics can also be given in gradient dynamics form [21,26,34].

To facilitate the model analysis, we introduce vertical and horizontal length scales $l = h_p$ and $L = (\gamma/\kappa)^{1/2} l$, respectively, with $l \ll L$, the time scale $\tau = L^2\eta_0/\kappa l$, and the energy scale $\kappa = k_B T l/a^3$. This gives dimensionless growth rate $\tilde{g} = g\tau$, osmotic mobility $\tilde{Q}_{\mathrm{osm}} = Q_{\mathrm{osm}}\tau\kappa/l^2$, and wettability parameter

$$W = \frac{A}{\kappa l^2} = \frac{A}{k_B T}\frac{a^3}{l^3} \quad (11)$$

that measures the relative strength of the wetting energy [35] as compared to the entropic free energy of mixing. Larger values of W correspond to a less wettable substrate and result in larger equilibrium contact angles.

Throughout the analysis, we fix the maximal amount of biomass that can be sustained by the substrate to $h^\star \phi_{\mathrm{eq}} = 60$, the equilibrium water concentration to $(1 - \phi_{\mathrm{eq}}) = 0.5$, and the ratio of the viscosities of biomass and fluid to $\eta_b/\eta_0 = 10\,000$ [36]. The biofilm spreading behavior is studied depending on the growth rate $\tilde{g}$, the wettability parameter W, and the osmotic mobility $\tilde{Q}_{\mathrm{osm}}$. Comparing with the typical biofilm height of 400 μm measured in Refs. [3,37–39] and using the viscosity and surface tension of water ($\eta_0 = 10^{-3}$ Pa s, $\gamma = 70$ mN/m) as well as the typical solvent or biomass length scale $a = 50$ nm, this results in the vertical length scale $l = h_p = 3$ μm, the lateral length scale $L = 85$ μm, and the time scale $\tau = 0.02$ s. With the above scales, a dimensionless expansion rate of 10^{-5} corresponds to a speed of 0.1–0.2 mm/h, which compares well with our measured expansion rate of 0.2 mm/h (see Fig. 2 in Ref. [18]). A wettability parameter $W = 8$ corresponds to an equilibrium contact angle of 5°, comparable to the dynamic contact angle measured in Ref. [3]. We analyze Eqs. (1)–(10) for a two-dimensional geometry (biofilm ridges instead of circular colonies) with no-flux boundaries employing numerical time simulations (finite element modular toolbox DUNE-PDELAB [40,41] as previously used in Refs. [26,34] and described in more detail in Ref. [18]) and continuation techniques [42] (software package AUTO-07P [43]).

Our model (1)–(10) reproduces the nonequilibrium transition between continuously spreading biofilms and arrested spreading: On the one hand, at relatively high wettability (lower W, Fig. 3 [top (a)] and [top (b)]), the biofilm initially rapidly swells vertically and horizontally until a stationary film height is reached. Subsequently, it

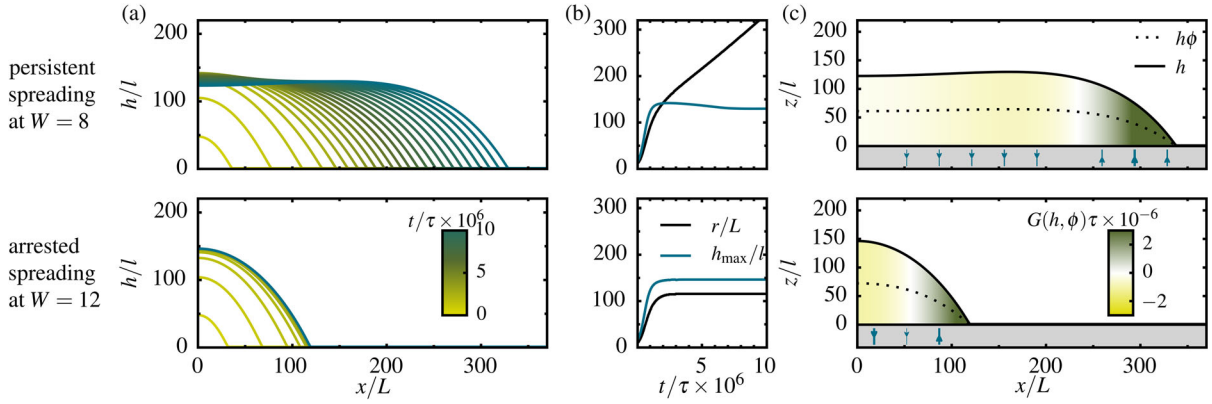

FIG. 3. Comparison of continuously spreading biofilms (top row, at $W = 8$) and arrested spreading of biofilms (bottom row, at $W = 12$). (a) Height profiles taken at equidistant times. (b) Time evolution of the biofilm extension $r(t)$ (solid black line) measured at the inflection point of the height profile and of the maximal film height $h_{\max}(t)$ (solid blue line). (c) Bioactivity and osmotic influx for biofilms at a late time when all transients have decayed. The shading within the film indicates the bioactivity $G(h,\phi)$. The direction and strength of the effective osmotic flux $\zeta(h,\phi)$ are represented by the direction and thickness of the blue arrows below the biofilm. Note that a time lapse of $10^6\tau$ corresponds to ≈5 h. Remaining parameters are $\tilde{g} = 2 \times 10^{-5}$ and $\tilde{Q}_{\mathrm{osm}} = 0.01$.

spreads only horizontally with a constant speed and shape of the biofilm edge. This qualitatively reproduces common experimentally observed behavior [2,4]. Figure 3 [top (c)] shows a snapshot of a spreading biofilm at a late time when all transients have decayed. Far from the advancing edges, the biofilm has reached the limiting amount of biomass, and the biomass concentration corresponds to the equilibrium value ϕ_{eq} so that all bioactive processes are in a dynamical equilibrium. At the edges, biomass growth takes place and causes an osmotic imbalance that results in a strong influx of water into the biofilm.

On the other hand, at lower wettability (larger W, Fig. 3 [bottom (a) and (b)]), biofilm spreading is arrested. Again, the biofilm initially rapidly swells; however, in contrast to the case of higher wettability, it soon evolves towards a steady profile of fixed extension and contact angle. Note that the steady biofilm drops are still bioactive–Fig. 3 [bottom (c)] shows that biomass is being produced at the biofilm edges where $G > 0$ and is degraded at the center where $G < 0$, as there the biomass exceeds the limiting amount $\phi_{eq} h^\star$. This is possible, as hydrodynamic and diffusive fluxes within the biofilm and osmotic fluxes between the agar and biofilm rearrange biomass and water such that their profiles are stationary. The spreading behavior in dependence of wettability parameter W and the biomass growth rate $\tilde{g}$ is summarized in the non-equilibrium phase diagram presented in Fig. 4. At constant $\tilde{g}$, corresponding, e.g., to a specific bacterial strain, spreading of the biofilm is arrested at low wettability (a high value of W). However, as adding a surfactant lowers the biofilm surface tension and, consequently, the parameter $W \sim \gamma$ [cf. Eqs. (3) and (11)], it can trigger a transition from a biofilm with arrested spreading to a continuously spreading biofilm—in agreement with the experimental results in Fig. 1 and Ref. [8].

This transition only slightly depends on the osmotic mobility $\tilde{Q}_{osm}$ (see Fig. 4), and one may consider the limiting case of an instantaneous osmotic solvent transfer between the agar and biofilm (i.e., $\tilde{Q}_{osm} \gg 1$). There, the model reduces to a one-variable model for the evolution of the biofilm height [44] and still reproduces all relevant experimental features. Even for this infinitely fast osmosis, the parameter region of arrested spreading is only slightly smaller than for finite $\tilde{Q}_{osm}$. This indicates that thermodynamic forces (surface forces, entropic forces) rather than time scales of transport and bioactive processes are dominant in the determination of the transition between steady and laterally expanding biofilms.

In summary, we have presented a simple model for the osmotic spreading of biofilms that grow at solid-air interfaces. The model adds bioactive processes into a hydrodynamic approach and explicitly includes wetting effects. In consequence, it has allowed us to study the interplay between biological growth processes and passive surface forces. Our results have confirmed within a thermodynamically consistent framework that wetting crucially affects the spreading dynamics of biofilms and has therefore provided a qualitative understanding of the experimentally observed transition between arrested and continuous spreading that occurs upon the addition of external surfactants in a surfactin-deficient *B. subtilis* strain.

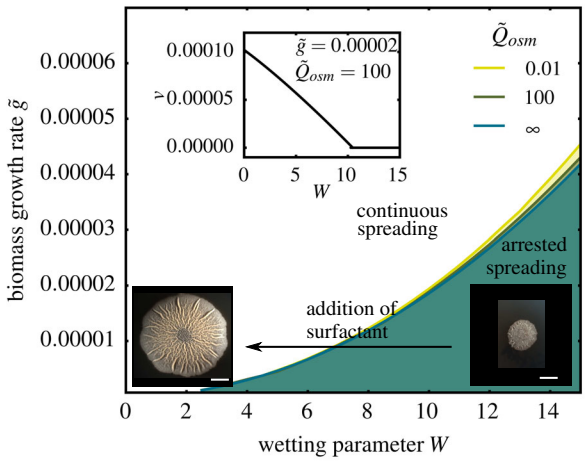

FIG. 4. Spreading behavior of the biofilm in the $\tilde{g}$-W parameter plane for various values of the osmotic mobility $\tilde{Q}_{osm}$ as indicated in the legend. In the shaded regions, biofilm spreading is arrested; i.e., it reaches a steady profile, while outside of this region, lateral spreading is not limited. The inset gives the dependence of spreading speed v on wettability W for $\tilde{g} = 2 \times 10^{-5}$ and $\tilde{Q}_{osm} = 0.01$. A speed of $v = 10^{-5}$ corresponds to an actual spreading speed of 0.1–0.2 mm/h, comparable to the experiment in Fig. 1 and in Ref. [2] (scale bar, 5 mm).

Our framework focuses on the description of the influence of surface tension and wetting properties on the spreading behavior of biofilms and neglects many processes that become important in mature colonies, such as cell differentiation or vertical gradients within the film. However, it is well suited to model the dynamics of the spreading biofilm edge. In future extensions, one may incorporate the autoproduction and dynamics of surfactants in the biofilm to consistently study the influence of Marangoni flows on the spreading dynamics [7,9,11]. As such flows are known to cause fingering instabilities in spreading surfactant-covered droplets [45], these mechanisms should be explored in connection to the branched structure described for some biofilm colonies. Furthermore, the modeling approach may easily be expanded to other setups such as biofilms that form at a liquid-solid interface under confinement as occurring in many practical applications [25].

We thank the lab of R. Losick at Harvard University for bacterial strains, the DAAD, Campus France (PHC PROCOPE Grant No. 35488SJ), and the CNRS (Grant No. PICS07343) for financial support. LIPhy is part of LabEx Tec 21 (Invest. l'Avenir, Grant No. ANR-11-LABX-0030).

*u.thiele@uni-muenster.de

[1] R. M. Donlan, Emerging Infect. Dis. **8**, 881 (2002).
[2] A. Seminara, T. Angelini, J. Wilking, H. Vlamakis, S. Ebrahim, R. Kolter, D. Weitz, and M. Brenner, Proc. Natl. Acad. Sci. U.S.A. **109**, 1116 (2012).
[3] W. Zhang, A. Seminara, M. Suaris, M. P. Brenner, D. A. Weitz, and T. E. Angelini, New J. Phys. **16**, 015028 (2014).
[4] G. E. Dilanji, M. Teplitski, and S. J. Hagen, Proc. R. Soc. B **281**, 20132575 (2014).
[5] P.-G. De Gennes, Rev. Mod. Phys. **57**, 827 (1985).
[6] D. Bonn, J. Eggers, J. Indekeu, J. Meunier, and E. Rolley, Rev. Mod. Phys. **81**, 739 (2009).
[7] R. Daniels *et al.*, Proc. Natl. Acad. Sci. U.S.A. **103**, 14965 (2006).
[8] V. Leclre, R. Marti, M. Bchet, P. Fickers, and P. Jacques, Arch. Microbiol. **186**, 475 (2006).
[9] M. Fauvart, P. Phillips, D. Bachaspatimayum, N. Verstraeten, J. Fransaer, J. Michiels, and J. Vermant, Soft Matter **8**, 70 (2012).
[10] W.-J. Ke, Y.-H. Hsueh, Y.-C. Cheng, C.-C. Wu, and S.-T. Liu, Front. Microbiol. **6**, 1017 (2015).
[11] T. Angelini, M. Roper, R. Kolter, D. A. Weitz, and M. P. Brenner, Proc. Natl. Acad. Sci. U.S.A. **106**, 18109 (2009).
[12] A. Be'er, R. S. Smith, H. Zhang, E.-L. Florin, S. M. Payne, and H. L. Swinney, J. Bacteriol. **191**, 5758 (2009).
[13] R. De Dier, M. Fauvart, J. Michiels, and J. Vermant, in *The Physical Basis of Bacterial Quorum Communication* (Springer, New York, 2015), pp. 189–204.
[14] A. Oslizlo, P. Stefanic, I. Dogsa, and I. Mandic-Mulec, Proc. Natl. Acad. Sci. U.S.A. **111**, 1586 (2014).
[15] J. van Gestel, H. Vlamakis, and R. Kolter, PLoS Biol. **13**, e1002141 (2015).
[16] P. D. Straight, J. M. Willey, and R. Kolter, J. Bacteriol. **188**, 4918 (2006).
[17] D. B. Kearns and R. Losick, Mol. Microbiol. **49**, 581 (2003).
[18] See Supplemental Material at http://link.aps.org/supplemental/10.1103/PhysRevLett.119.078003 for a detailed description of the procedure for the numerical time simulations as well as for the growth experiments. Furthermore, images of the colonies taken at subsequent days after incubation are shown. The growth rate is provided for both strains with or without the addition of surfactant.
[19] U. Thiele, D. V. Todorova, and H. Lopez, Phys. Rev. Lett. **111**, 117801 (2013).
[20] U. Thiele, Eur. Phys. J. Spec. Top. **197**, 213 (2011).
[21] X. Xu, U. Thiele, and T. Qian, J. Phys. Condens. Matter **27**, 085005 (2015).
[22] Q. Wang and T. Zhang, Solid State Commun. **150**, 1009 (2010).
[23] I. Klapper and J. Dockery, SIAM Rev. **52**, 221 (2010).
[24] H. Horn and S. Lackner, in *Productive Biofilms*, Vol. 146, edited by K. Muffler and R. Ulber (Springer, New York, 2014), pp. 53–76.
[25] C. Picioreanu and M. C. M. Van Loosdrecht, in Use of mathematical modelling to study biofilm development and morphology. Chapter 22., *Biofilms in Medicine, Industry and Environmental Biotechnology characteristics: Analysis And Control* (IWA Publishing, United Kingdom, 2003), pp. 413–438.
[26] S. Trinschek, K. John, and U. Thiele, AIMS Mater. Sci. **3**, 1138 (2016).
[27] J. Ward and J. King, J. Eng. Math. **73**, 71 (2012).
[28] U. Thiele, in *Thin Films of Soft Matter*, edited by S. Kalliadasis and U. Thiele (Springer, Wien, 2007), pp. 25–93.
[29] L. Hall-Stoodley, J. W. Costerton, and P. Stoodley, Nat. Rev. Microbiol. **2**, 95 (2004).
[30] I. Sutherland, Microbiology **147**, 3 (2001).
[31] P. C. Lau, J. R. Dutcher, T. J. Beveridge, and J. S. Lam, Biophys. J. **96**, 2935 (2009).
[32] L. Dietrich, C. Okegbe, A. Price-Whelan, H. Sakhtah, R. Hunter, and D. Newman, J. Bacteriol. **195**, 1371 (2013).
[33] The explicit form of $f_{\mathrm{mod}}(h,\phi)$ is chosen as

$$f_{\mathrm{mod}}(h,\phi) = \left(1 - \frac{\phi_{\mathrm{eq}} h_u}{\phi h}\right)[1 - \exp(\phi_{\mathrm{eq}} h_p - \phi h)] \qquad (12)$$

with the minimal biomass amount $\phi_{\mathrm{eq}} h_u$ that is needed for bacterial proliferation. Other choices for $f_{\mathrm{mod}}(h,\phi)$ with the same fixed point structure do not change the results qualitatively.
[34] M. Wilczek, W. Tewes, S. V. Gurevich, M. H. Köpf, L. Chi, and U. Thiele, J. Phys. Condens. Matter **29**, 014002 (2017).
[35] L. M. Pismen and U. Thiele, Phys. Fluids **18**, 042104 (2006).
[36] J. N. Wilking, T. E. Angelini, A. Seminara, M. P. Brenner, and D. A. Weitz, MRS Bull. **36**, 385 (2011).
[37] H. Vlamakis, C. Aguilar, R. Losick, and R. Kolter, Genes Dev. **22**, 945 (2008).
[38] X. Wang, G. Wang, and M. Hao, Comput. Math. Methods Med. **2015**, 581829 (2015).
[39] X. Wang *et al.*, Applied Microbiology and Biotechnology **100**, 4607 (2016).
[40] P. Bastian, M. Blatt, A. Dedner, C. Engwer, R. Klöfkorn, R. Kornhuber, M. Ohlberger, and O. Sander, Computing **82**, 121 (2008).
[41] P. Bastian, M. Blatt, A. Dedner, C. Engwer, R. Klöfkorn, R. Kornhuber, M. Ohlberger, and O. Sander, Computing **82**, 103 (2008).
[42] H. A. Dijkstra, F. W. Wubs, A. K. Cliffe, E. Doedel, I. F. Dragomirescu, B. Eckhardt, A. Y. Gelfgat, A. Hazel, V. Lucarini, A. G. Salinger, E. T. Phipps, J. Sanchez-Umbria, H. Schuttelaars, L. S. Tuckerman, and U. Thiele, Commun. Comput. Phys. **15**, 1 (2014).
[43] E. J. Doedel and B. E. Oldeman, *AUTO-07P: Continuation and Bifurcation Software for Ordinary Differential Equations* (Concordia University, Montreal, 2007).
[44] If the influx of water is fast as compared to biomass growth but not as fast as the hydrodynamic fluxes, one can reduce the model to an effective description of the biofilm height, as the large biofilm droplets are always in "osmotic equilibrium" $\mu_s = \mu_{\mathrm{agar}}$ with the substrate on the time scale of the biomass growth with

$$\zeta(h,\phi) = \frac{1}{1-\phi_{\mathrm{eq}}} G(h,\phi).$$

The evolution equation for the total height reduces to

$$\partial_t h = \nabla \cdot \left[\frac{h^3}{3\hat{\eta}} \nabla(\partial_h f_w - \Delta h)\right] + \frac{1}{1-\phi_{\mathrm{eq}}} G(h, 1-\phi_{\mathrm{eq}})$$

with a constant viscosity $\hat{\eta} = \phi_{\mathrm{eq}} + k_\eta(1-\phi_{\mathrm{eq}})$.
[45] O. K. Matar and S. M. Troian, Phys. Fluids **11**, 3232 (1999).